Available online at www.sciencedirect.com
SCIENCE DIRECT
Developmental Biology 293 (2006) 540–554
DEVELOPMENTAL BIOLOGY
www.elsevier.com/locate/ydbio

Genomes & Developmental Control

Comprehensive microarray analysis of Hoxa11/Hoxd11 mutant kidney development

Kristopher Schwab [a], Heather A. Hartman [b], Hung-Chi Liang [a], Bruce J. Aronow [c], Larry T. Patterson [b], S. Steven Potter [a,*]

[a] Division of Developmental Biology, Children's Hospital Medical Center, 3333 Burnet Avenue, Cincinnati, OH 45229, USA
[b] Division of Nephrology, Children's Hospital Medical Center, 3333 Burnet Avenue, Cincinnati, OH 45229, USA
[c] Division of Bioinformatics, Children's Hospital Medical Center, 3333 Burnet Avenue, Cincinnati, OH 45229, USA

Received for publication 13 December 2005; revised 2 February 2006; accepted 16 February 2006

Abstract

The Hox11 paralogous genes play critical roles in kidney development. They are expressed in the early metanephric mesenchyme and are required for the induction of ureteric bud formation and its subsequent branching morphogenesis. They are also required for the normal nephrogenesis response of the metanephric mesenchyme to inductive signals from the ureteric bud. In this report, we use microarrays to perform a comprehensive gene expression analysis of the Hoxa11/Hoxd11 mutant kidney phenotype. We examined E11.5, E12.5, E13.5 and E16.5 developmental time points. A novel high throughput strategy for validation of microarray data is described, using additional biological replicates and an independent microarray platform. The results identified 13 genes with greater than 3-fold change in expression in early mutant kidneys, including Hoxa11s, GATA6, TGFbeta2, chemokine ligand 12, angiotensin receptor like 1, cytochrome P450, cadherin5, and Lymphocyte antigen 6 complex, Iroquois 3, EST A930038C07Rik, Meox2, Prkcn, and Slc40a1. Of interest, many of these genes, and others showing lower fold expression changes, have been connected to processes that make sense in terms of the mutant phenotype, including TGFbeta signaling, iron transport, protein kinase C function, growth arrest and GDNF regulation. These results identify the multiple molecular pathways downstream of Hox11 function in the developing kidney.

Keywords: Kidney development; Microarrays; Hox genes; Laser capture microdissection; Metanephric mesenchyme; Ureteric bud; Morphogenesis

Introduction

The kidney is an excellent model system for studying the principles of organogenesis. The developing kidney exhibits many interesting processes, including establishment of an early metanephric field by tissue interactions, budding, reciprocal inductive interactions between ureteric bud (UB) and metanephric mesenchyme (MM), stem cell growth and differentiation, and conversion of mesenchyme into epithelia. In addition, there is branching morphogenesis, apoptosis, fusion (nephrons to collecting ducts), and proximal–distal segmentation along the length of the nephron [for review, see (Davies and Bard, 1998)]. Metanephric, or adult, kidney development begins in the mouse at around embryonic day 11.0 (E11.0) as the UB grows from the nephric duct and invades the MM. The UB induces the cells of the MM to condense, epithelialize, and form renal vesicles, each of which develops into a functional nephron containing a glomerulus, proximal tubule, loop of Henle and distal tubule. Of particular importance, kidney morphogenesis can be readily studied in organ culture (Saxen and Lehtonen, 1987).

We have made significant advances in understanding the genetic regulation of kidney organogenesis (Bouchard, 2004; Yu et al., 2004). Hox genes play important roles in this process. These transcription factor-encoding genes often occupy high level positions in the genetic hierarchy of development. It is interesting that a total of 27 Hox genes show specific domains of expression in the developing kidney (Patterson and Potter, 2004). Mutations in the Hoxa11, Hoxc11 and Hoxd11 closely

* Corresponding author. Fax: +1 513 636 4317.
E-mail address: steve.potter@cchmc.org (S.S. Potter).

0012-1606/$ - see front matter © 2006 Elsevier Inc. All rights reserved.
doi:10.1016/j.ydbio.2006.02.023

related paralogous genes reveal that they have redundant functions in several aspects of kidney development (Davis et al., 1995; Patterson et al., 2001; Wellik et al., 2002). These three genes are expressed in the early MM, and the combined mutation of all three gives a loss of GDNF synthesis and failure of the UB to form (Wellik et al., 2002). A hypomorphic mutant allele combination, with mutations in Hoxa11 and Hoxd11 but not Hoxc11, results in a MM that does not properly drive branching morphogenesis of the UB, and in turn does not respond correctly to UB signals (Patterson et al., 2001). These results indicate that the Hox11 paralogs play crucial roles in several stages of kidney development. There are still important gaps, however, in our understanding of the downstream genetic pathways regulated by these Hox genes.

The microarray is a useful tool for gaining deeper insight into the genetic program of kidney development. Microarrays can provide an important gene discovery function, identifying all genes expressed in the developing kidney and cataloging changes that occur over time. In addition, they allow an impartial global view of altered gene expression profiles in mutant developing kidneys. Instead of looking at just a few selected marker genes by in situ hybridization, it is now possible to conduct an unbiased and universal analysis of gene expression patterns in mutants.

In this paper, we extend the previous microarray studies of normal kidney development, and then use this wild type baseline to analyze the altered gene expression patterns of the Hoxa11/Hoxd11 mutant kidney. We used Affymetrix MOE430 oligonucleotide microarrays to examine gene expression profiles of the complete normal kidney at E12.5, E13.5, E16.5 and adult. In addition, we determined the gene expression patterns of the E11.5 MM and UB, using both laser capture microdissection and manual microdissection to isolate tissues, thereby identifying over 1500 genes with strong differential expression. These results serve to identify the gene expression networks and signaling pathways active in these kidney primordia. Finally, we performed an extensive microarray dissection of the altered gene expression patterns present in Hoxa11/Hoxd11 double mutant kidneys. Several developmental time points were examined, including E11.5, E12.5, E13.5 and E16.5. To allow a more robust microarray analysis of the mutant differences we combined independent data from the Affymetrix and Illumina microarray platforms. The results identify a battery of downstream genes that provide deeper insight into the molecular mechanisms of Hox11 function in kidney development.

Methods

Breeding and genotyping Hoxa11/Hoxd11 mutant mice

Hoxa11 and Hoxd11 mutant mice were previously described (Davis et al., 1995; Patterson et al., 2001; Small and Potter, 1993). The colony was maintained on a mixed genetic background of four strains of mice (129, C57, C3H and CF1). Hoxa $11^{+/-}$, Hoxd$11^{+/-}$ double heterozygous female mice have uterine defects that severely limit reproductive capacity (Hsieh-Li et al., 1995). We therefore isolated zygotes from double heterozygote crosses, with superovulated females, and transferred them to pseudo-pregnant surrogate wild type CD-1 females (Nagy, 2003). Noon of the day when the vaginal plug was observed was considered embryonic day 0.5 (E0.5). All mice and embryos were genotyped as previously described (Patterson et al., 2001). This study focuses on Hoxa11, Hoxd11 double homozygous mutant mice.

Tissue dissections

Wild type tissues from E12.5 and older were obtained from outbred CD-1 mice. Whole embryonic kidneys and urogenital ridges were dissected in ice-cold PBS then either frozen at −80°C, or quick-frozen in Tissue-Tek® OCT compound (Sakura, Torrence, CA) using liquid nitrogen cooled 2-methylbutane. MM and UBs, up to T-shaped stage, were isolated by treating dissected E11.5 kidneys with 0.5 mg/ml collagenase B (Roche, Indianapolis, IN), in D-MEM (Invitrogen, Carlsbad, CA) for 30 min at 37°C and carefully dissecting the mesenchyme from the UB, followed by storage at −80°C.

Laser-capture microdissection

E11.5 whole embryos were frozen in OCT. For later time points the kidneys were removed and frozen in OCT. Serial sections (7μ) were made using a Microm HM 550 cryostat (Richard-Allan Scientific, Kalamazoo, MI), collected on Fisher Superfrost plus precleaned slides (Hampton, NH), and stored at −80°C. Alternate sections were hematoxylin and eosin stained and used to help identify the UB and MM. For LCM, the remaining sections were air dried at room temperature for 3 min, acetone fixed for 2 min, rinsed in ice cold 1/10 PBS for 3 min and then dehydrated in 75%, 95%, 100%, 100% ethanol, followed by two 5-min rinses with xylene. Laser capture microdissection was performed using the Arcturus Pixcell II system, according to Arcturus protocols (Mountain View, California).

RNA isolation and target RNA amplification

Total RNA from wild type and mutant whole kidneys was prepared using the Stratagene Absolutely RNA Nanoprep Kit (La Jolla, CA) and amplified as previously described (Schwab et al., 2003). Target RNA was then hybridized to both the MOE430A and MOE430B Genechips (Affymetrix, Santa Clara, CA). Microarray analysis of each stage was performed in biological duplicate using either 30 ng or 100 ng of starting total RNA.

Each microarray hybridization represented a biological replicate, using an independent biological sample. We pooled 3–9 wild type UB for each sample, and 2–4 MM for each sample. Mutant E11.5 MM was not pooled.

LCM RNA was prepared using the RNeasy Micro Kit (Qiagen, Valencia, CA), with 30 ng poly-inosine carrier (Epicentre, Madison, WI) added to the RLT buffer. Target RNA was prepared using the TargetAmp™ 2-Round aRNA Amplification Kit 1.0 (Epicentre, Madison, WI), and hybridized to Affymetrix MOE430_v2 microarrays.

To validate the Affymetrix results, total RNA was isolated from HoxA11/D11 null and normal E13.5 whole kidneys or E11.5 MM, amplified using the Epicentre TargetAmp™ 2-Round aRNA Amplification Kit (Madison, WI) and hybridized to Sentrix MouseRef-8 Beadchip microarrays (Illumina, San Diego, CA) containing over 24,000 probes.

Gene expression profile analysis

Affymetrix raw data in the CEL file format was normalized using RMA Express 0.2 (Bolstad et al., 2003) and analyzed using Genespring 7.0. Illumina raw signal data was imported into the Affymetrix MOE430 genome on basis of gene symbol for analysis. Wild type whole developing kidney samples were normalized to adult samples. Normal E11.5 MM samples were normalized to E11.5 UB. HoxA11/D11 null samples were normalized to the corresponding wild type control. Hierarchical clusters were generated using the Pearson Correlation Function. All microarray data are available from Signet (http://cypher.cchmc.org:1104/servlet/GeNet, login as "Guest, select MOE430 genome, data contained in "SPotter/Schwab et al. 2005 folders") allowing interactive analysis of the data, through other public databases (GEO, GUDMAP), and will be provided upon request.

QPCR validation of microarray changes

Total RNA was obtained and DNAse 1 treated from separate E13.5 Hoxa11/d11 (n = 4) and control kidneys (n = 3) using Stratagene Absolutely RNA Microprep Kit (La Jolla, CA). cDNA was generated using random hexamers according to conventional protocols (Invitrogen, Carlsbad, Ca). The following primers were generated specifically to the sequence obtained from the Affymetrix probe set: Actb (TTGCTGACAGGATGCAGAAG, ACATCTGCTGGAAGGTGGAC), Cxcl12 (GTCTAAGCAGCGATGGGTTC, TAGGAAGCTGCCTTCTCCTG), HoxA11s (TGTCCTGGAGGAAGGAGAA, ATCACCACCATTGGGAGGT), Pdgfrb (AGCAAGAGTGGCAGAGAAGG, TAATCCCGTCAGCATCTTCC), Slit3 (CGTGGAAGAGGTGGAGAGAC, AGAGGTTCCATGTGGCTGTT), and Tgfb2 (GAAATACGCCCAAGATCGAA, TGTCACCGTGATTTTCGTGT) using Primer3 software (Rozen and Skaletsky, 2000). Relative quantitative PCR was performed according to the conventional SYBR Green protocol (Stratagene) using the Stratagene Mx3000p QPCR system. Dissociation curve and agarose gel analysis of each primer set were used to insure specificity of the amplicon. All data were normalized to an internal housekeeping control (Actb) and analyzed using the 2(-Delta Delta C(T)) method (Livak and Schmittgen, 2001).

Results

Microarray comparisons of gene expression profiles of wild type E12.5, E13.5, E16.5 and adult kidneys

We used Affymetrix MOE430 microarrays to examine gene expression patterns of the normal developing kidney at E12.5, E13.5, E16.5 and adult. These oligonucleotide arrays carry over 48,000 probe sets and monitor expression levels of over 20,000 genes. A high stringency analysis of the data identified 2793 genes that showed a strong change in expression level as a function of developmental time. The heat map in Fig. 1 illustrates the patterns observed. The gene expression profiles of E12.5 and E13.5 kidneys were very similar, while at E16.5 a significant block of genes showed altered expression. Expression levels were normalized to that of the adult kidney, shown in the right two lanes. All data and gene lists are available from the Signet server (see Methods).

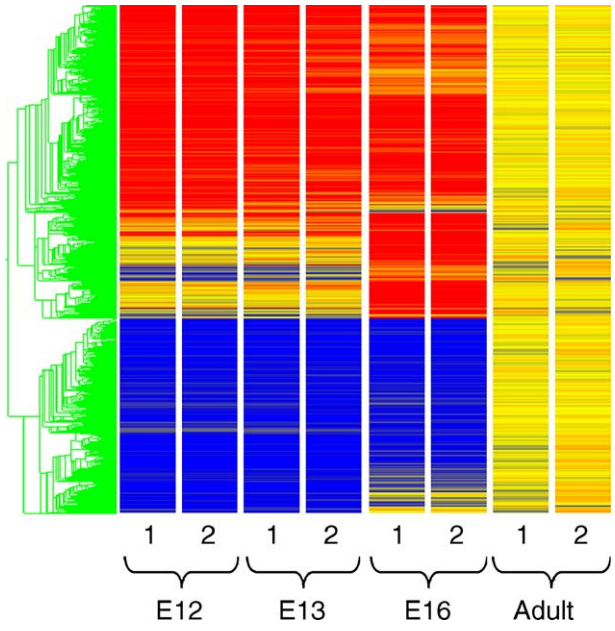

Fig. 1. Heat map showing 2793 genes clustered according to expression during kidney development. Developmental times include E12.5, E13.5, E16.5 and adult. Expression levels were normalized to the adult kidney. Red shows elevated, blue indicates reduced, and yellow shows unchanged expression. Only genes with greater than 3-fold change are included. Complete gene lists and analysis tools are available online (see Methods).

Gene expression profiles of the E11.5 MM and UB

The MM and UB represent the embryonic precursors of the adult kidney. At E11.5, the UB has invaded the MM. A series of reciprocal inductive interactions drive the mesenchyme to convert to epithelia and form nephrons, while the bud undergoes branching morphogenesis and forms the collecting ducts.

To better understand the distinct properties of the UB and MM, we defined their gene expression profiles. The UB is a discrete structure and was cleanly purified by manual microdissection following enzymatic treatment to dissociate the surrounding mesenchyme. The MM, with a more poorly defined outer border at this stage of development, was isolated by both manual microdissection and by laser capture microdissection. To provide a UB-MM comparison with great statistical power, we examined a total of four UB and seven MM biological replicates.

The resulting microarray data showed a high degree of reproducibility. The scattergraph in Fig. 2A compares the gene expression patterns of two MM samples purified by laser capture microdissection. If each gene showed exactly the same expression in both samples there would be a single line at 45 degrees. There is some scatter, with about 1% (526) of the >48,000 probe sets giving more than a 3-fold difference (green lines) in expression level between the two samples. This is likely due to a combination of biological variation, sampling error during LCM, and noise resulting from the two round target amplification procedure required because of the small amount of starting RNA. This noise is eliminated in the analysis by examining multiple biological replicates and requiring consistent change. Fig. 2B compares MM isolated by LCM versus mesenchyme isolated by manual microdissection, showing a similar level of scatter to that seen in Fig. 2A. Interestingly, there was significantly less scatter in pair-wise comparisons of UB samples (Fig. 2C), with less than 0.1% of probe sets (56) showing over a 3-fold difference in expression level. Most striking, however, was the large number of genes with dramatic differences in expression when comparing the UB and MM (Fig. 2D).

A stringent analysis of the UB and MM microarray data was performed. Using rigorous criteria requiring an average fold change of at least three, with Benjamini and Hochberg false discovery rate multiple testing correction, and a t test of $P < 0.05$, we identified 1518 differently expressed genes. This is illustrated in the heat map of Fig. 3. These numbers are higher than previously reported (Schwab et al., 2003) because of improved purification protocols, more comprehensive microarrays, and the use of a considerably larger number of microarrays (11 vs. 4), lending greater statistical power to the analysis.

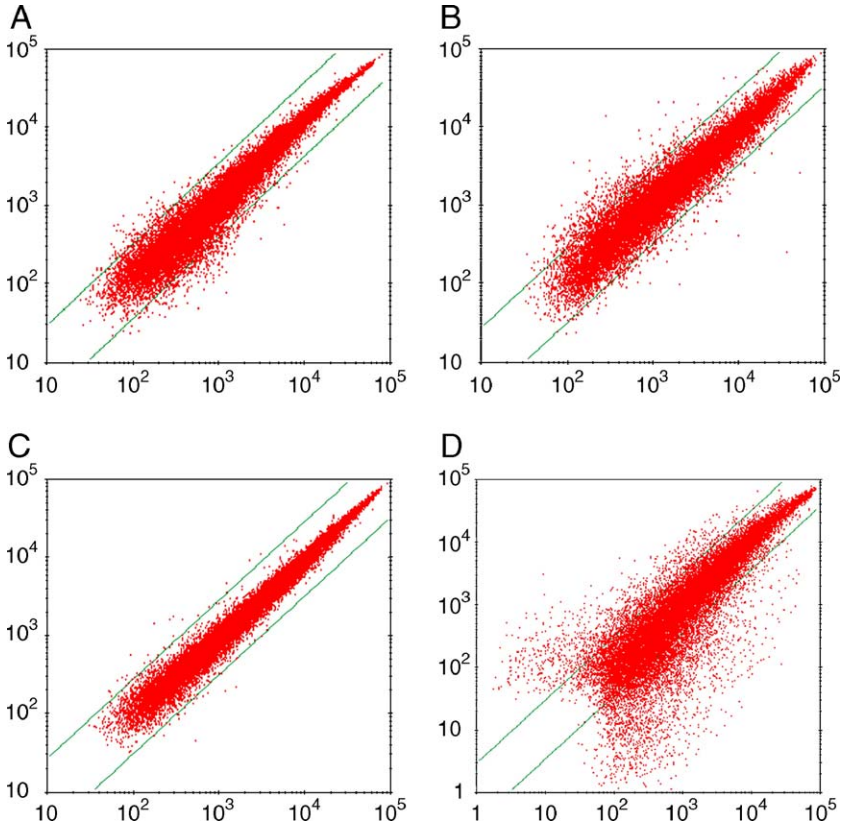

Fig. 2. Scattergraphs of E11.5 UB and MM microarray data. (A) Biological replicates of E11.5 MM purified by LCM. (B) Comparison of manually dissected and LCM isolated E11.5 MM. (C) Biological replicates of manually dissected E11.5 UB. (D) Comparison of UB and MM samples. Note the good reproducibility of MM data, whether isolated by manual microdissection or LCM, and the still higher reproducibility of the UB data. The MM-UB comparison, in contrast, shows striking differences. Green lines mark the 3-fold difference boundary. Each dot represents one probeset that has been called by the GCOS software as "Present" in each microarray, except in D in which at least one probeset must be called "Present."

Examination of the list of differently expressed genes identifies many interesting genes not previously implicated in early kidney development. In addition, 63 genes that have been previously shown to exhibit restricted UB or MM expression are found on the list of 1518 genes. These genes are included in Table 1 along with references documenting discrete expression. Of interest, in each case the microarray data is consistent with the previous expression study. This universal agreement of the microarray data with previous in situ hybridization studies provides an important measure of validation. The UB-MM specific expression patterns of GDNF, Ret, Hoxa11, Hoxc10, Hoxd10, Hoxa10, Wnt9b, Wnt4, Wnt11, Six2, Wt1, Foxc1, Lhx1 and 50 other genes were all correctly called by the microarrays. In addition, Table 1 lists other selected genes ranked according to fold difference in expression. These genes encode cytokines, receptors, and several categories of transcription factors and growth factors, of potential importance in programming the early functions of these two structures.

Analysis of Hoxa11/d11 mutant kidneys

This microarray atlas of gene expression patterns in the normal developing kidney provides a baseline that can be used for the global analysis of altered gene expression patterns in mutants. Previous studies have shown that the Hox11 paralogous genes play important, yet redundant roles in several phases of kidney development (Davis et al., 1995; Patterson et al., 2001; Wellik et al., 2002). To better understand the molecular level perturbations present in the mutant kidneys, we performed an exhaustive microarray analysis. We focused on the Hoxa11/Hoxd11 double homozygous mutant. These mice show a severe kidney phenotype, with reduced branching morphogenesis of the collecting duct system and altered gene expression patterns, as defined by in situ hybridization, during nephrogenesis (Patterson et al., 2001). Further removal of the Hoxc11 gene results in very early arrest of kidney development (Wellik et al., 2002), precluding the study of later developmental functions of this gene group.

E12.5/E13.5 wild type-Hoxa11/d11 mutant comparison

Our first comparisons of wild type and Hoxa11/d11 mutant used Affymetrix MOE430 microarrays and examined E12.5, E13.5 and E16.5 developmental time points, each in biological duplicate. As might be expected, the gene expression profiles of the wild type and Hoxa11/d11 mutant kidneys were much more similar than seen for the wild type UB-MM comparison. Lowering the stringency of the analysis to find the lower fold

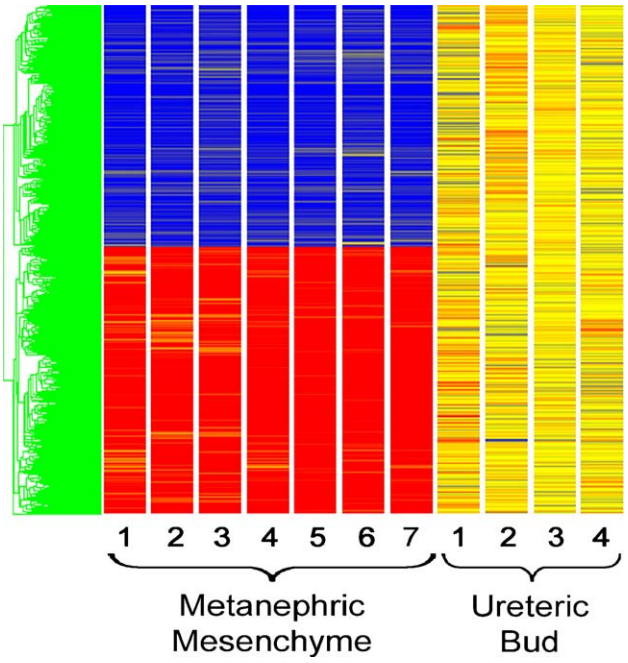

Fig. 3. Heat map showing 1518 genes clustered according to differential expression in E11.5 UB and MM. The MM expression levels were normalized to UB. The upper blue cluster represents 800 genes with decreased expression in the MM. The lower red cluster shows 718 genes with higher expression levels in the MM. Note the high reproducibility of the expression differences across all samples.

gene expression changes present in the mutants resulted in many artifact difference calls, as shown by real time PCR validation (data not shown).

To improve the discriminatory power of the study, we repeated the microarray analysis of the E13.5 wild type and mutant kidneys, this time using the Illumina beaded array platform. This provided additional microarray data, making the statistical comparison stronger, and it added more biological samples, as biological replicates were performed, further helping to remove biological noise. In addition, it gave a new microarray perspective, since an independent microarray system was used. Three normal and two mutant E13.5 kidneys were examined with Illumina. This gave a total of nine microarrays for the E13.5 comparison, with five Illumina and four Affymetrix. These data were analyzed with GeneSpring 7.0, setting the screen parameters at non-parametric test (Welch *t* test) $P < 0.05$, using Benjamini and Hochberg multiple testing correction, fold change >1.5, and a minimum raw expression of 400 in at least two samples to remove genes with very low expression levels. This resulted in a list of 467 genes (Supplementary Figure S1).

To further strengthen the analysis, we combined the data from the wild type-mutant comparisons at E12.5 and 13.5. These two time points showed similar wild type gene expression profiles (Fig. 1). A comparable stringency analysis of the E12.5 data was performed, using four Affymetrix MOE430 microarrays, and deleting the multiple testing correction, because of the smaller number of microarrays used. The resulting gene list was used to determine the set of overlapping genes, with different expression levels in both the E12.5 and E13.5 wild type versus mutant comparisons. This gave a list of 122 probe sets, representing 107 different genes (Table 2), with relative expression levels in the 17 microarrays shown in the heat map of Fig. 4. These genes gave consistent expression level differences in both the E12.5 and E13.5 wild type versus mutant comparisons. In addition, many showed similar expression changes in the E16.5 wild type and mutant kidneys (Fig. 4).

It is interesting that the gene showing the greatest change in expression in the Hoxa11/d11 mutants was the Hoxa11 antisense transcript. We have previously shown that the Hoxa11 gene gives rise to both sense and antisense transcripts (Hsieh-Li et al., 1995). The targeting of the Hoxa11 gene created a deletion including the homeobox region (Small and Potter, 1993), which clearly reduced antisense transcription. The Affymetrix microarrays also identified a significant reduction of Hoxa11 sense transcripts in the mutants (−6.3-fold at E12.5, −6.4 at E13.5 and −5.8 at E16.5). This difference, however, was not detected by the Illumina microarrays, which reported very low expression of Hoxa11 even in the wild type (raw signals of 70 to 160), so this gene did not make the final list. This illustrates that the two microarray platforms show gene specific detection differences. In general, we observed that both platforms provided excellent concordant expression level analysis for most genes. But a few genes were better assayed by one system, and other genes by the other. By requiring both types of microarrays to observe a change it is clear that some genuine expression changes, such as the Hoxa11 sense transcript, will be lost. The Hoxd11 gene was targeted in a different manner, not by deletion but by the insertion of a Neo selectable marker. Neither microarray system found a change in expression level of this gene, suggesting that the insertion did not significantly alter transcript abundance.

It is also interesting to note that 15 of the genes called differently expressed are represented by duplicate probe sets on the Affymetrix microarrays. That is, the probe set list of 122 includes only 107 different genes. The fold changes called by these independent probes sets in this combined data set show excellent agreement. These include, in alphabetical order, angiotensin receptor like-1 (fold changes of 2.5, 3.1), carbonic anhydrase 4 (−1.9, −2.1), elastin microfibril interfacer 1 (2.2, 2.2), EST AI450540 (1.6, 2.2), Fibrillin 1 (2.5, 2.0), GATA6 (3.9, 3.0), high mobility group box 1 (−1.6, −1.8), insulin-like growth factor binding protein 4 (2.0, 1.8), Lipoma HMGIC fusion partner-like 2 (1.7, 1.6), mastermind like 1 (2.3, 1.7), pdgf receptor beta (2.6, 2.1), Procollagen, type V, alpha 1 (2.5, 1.9), Procollagen, type XVIII, alpha 1 (2.3, 2.0), Procollagen, type XXIII, alpha 1 (2.3, 2.0).

To further test the validity of the resulting gene list we performed real time PCR for five genes. The results are shown in Fig. 5. For all five genes a significant difference in gene expression was confirmed, in the direction predicted by microarrays. The fold change agreement between microarray

Table 1
Select transcription factor or signaling pathway transcripts ranked by average fold difference between the E11.5 MM and UB

Gene name	MM or UB enrichment	Fold change	Reference	Gene name	MM or UB enrichment	Fold change	Reference
Foxd1	MM	81.3	(Hatini et al., 1996)	Pou3f3	UB	52.9	
Hoxc10	MM	71.4	(Patterson and Potter, 2004)	Crlf1	UB	41.0	(Schmidt-Ott et al., 2005)
Hoxd10	MM	61.3	(Patterson and Potter, 2004)	Cdh1	UB	29.6	(Klein et al., 1988)
Meis1	MM	57.1		Emx2	UB	27.8	(Miyamoto et al., 1997)
Gdnf	MM	51.5	(Moore et al., 1996; Pichel et al., 1996; Sanchez et al., 1996)	Calcr	UB	27.5	
Eya1	MM	49	(Kalatzis et al., 1998)	Sostdc1	UB	24.9	(Schmidt-Ott et al., 2005)
Isl1	MM	47.4		Lhx1	UB	22.5	(Kobayashi et al., 2005)
Eya4	MM	46.5		Cdh16	UB	20.2	
Pdgfra	MM	45.5	(Seifert et al., 1998)	Wnt9b	UB	18.8	(Carroll et al., 2005; Kobayashi et al., 2005)
Itga8	MM	45	(Muller et al., 1997)	Itk	UB	18.1	
Sall1	MM	44.6	(Nishinakamura et al., 2001)	Elf5	UB	15.5	
Tgfbi	MM	38.2	(Schwab et al., 2003)	Sim1	UB	15.3	
Foxc2	MM	38	(Kume et al., 2000b)	Fgfr4	UB	14.8	(Stark et al., 1991)
Hoxa10	MM	37.9	(Patterson and Potter, 2004)	Npnt	UB	14.4	(Brandenberger et al., 2001)
Tbx18	MM	35.2		Ros1	UB	13.8	(Tessarollo et al., 1992)
Tcf21	MM	33.3	(Quaggin et al., 1999)	Tcf2	UB	13.6	
Hoxa9	MM	32.1	(Patterson and Potter, 2004)	Tbx3	UB	13.1	
Hoxc8	MM	28.4	(Patterson and Potter, 2004)	Gata3	UB	12.1	(Labastie et al., 1995; Lim et al., 2000)
Foxc1	MM	24.9	(Kume et al., 2000b)	Igfbp1	UB	11.0	
Csf1r	MM	24.9		Irf6	UB	10.6	
Agtr2	MM	24		Igfbp2	UB	10.4	(Schmidt-Ott et al., 2005)
Wt1	MM	20.8	(Kreidberg et al., 1993; Ryan et al., 1995)	Wnt6	UB	10.1	(Itaranta et al., 2002)
Twist2	MM	17.8		Shh	UB	10.0	(Yu et al., 2002)
Foxp2	MM	16		Hoxd1	UB	9.4	(Patterson and Potter, 2004)
Prrx1	MM	15.7		Lama1	UB	9.2	(Schmidt-Ott et al., 2005)
Frzb	MM	13.8		Cxcl14	UB	9.1	(Schmidt-Ott et al., 2005)
Meox2	MM	13.3		Tcf7	UB	8.5	
Cdh11	MM	12.7	(Cho et al., 1998)	Fgf12	UB	8.4	
Hand2	MM	12.5		Mia1	UB	7.9	(Schwab et al., 2003)
Six2	MM	12.5	(Oliver et al., 1995)	Socs2	UB	7.8	
Meox1	MM	12.1	(Candia et al., 1992)	Tnfrsf19	UB	7.4	
Pdgfrb	MM	11.4	(Seifert et al., 1998)	Klf5	UB	7.4	
Cart1	MM	11.4		Sema4d	UB	7.3	
Hoxa11s	MM	10.7	(Hsieh-Li et al., 1995)	Pgr	UB	6.8	
Reln	MM	10.6		Ret	UB	6.7	(Durbec et al., 1996; Schuchardt et al., 1994)
Wnt4	MM	9.3	(Kispert et al., 1998; Stark et al., 1994)	Wnt11	UB	6.7	(Majumdar et al., 2003)
Nr2f2	MM	8.8		Kitl	UB	6.6	(Schmidt-Ott et al., 2005)
Bmp4	MM	8.7	(Miyazaki et al., 2000)	Epha1	UB	6.3	
Gata6	MM	8.6		Fzd5	UB	6.1	
Twist1	MM	8.5		Sall4	UB	6.1	
Itga8	MM	8.3	(Muller et al., 1997)	Fzd6	UB	6.1	
Tgfb2	MM	8.1	(Plisov et al., 2001)	Sox6	UB	6.0	
Cxcl4	MM	8.1		Pou3f4	UB	6.0	
Cxxc4	MM	7.9		Emb	UB	5.9	(Fan et al., 1998)
Igf1	MM	7.8		Lama5	UB	5.7	
Calcrl	MM	7.3		Sema3c	UB	5.7	
Hoxc4	MM	6.7	(Patterson and Potter, 2004)	Tbx2	UB	5.6	
Ace2	MM	6.4		Fstl5	UB	5.3	
Tbx18	MM	6.2		Spry1	UB	5.3	(Basson et al., 2005)
Tgfb3	MM	6		Fzd8	UB	5.1	
Cxcl7	MM	5.8		Irx3	UB	4.8	
Foxd2	MM	5.5	(Kume et al., 2000a)	Cdh3	UB	4.7	
Tek	MM	5.4		Sema4f	UB	4.7	
Tgfb1i1	MM	4.8	(Brunskill et al., 2001)	Tgfa	UB	4.7	
Itga6	MM	4.8		Bspry	UB	4.6	
Prrx2	MM	4.8		Cd9	UB	4.6	
Tie1	MM	4.6	(Loughna et al., 1997)	Neuregulin 3	UB	4.5	
Cxcl12	MM	4.6		Hoxd8	UB	4.5	(Patterson and Potter, 2004)

(continued on next page)

Table 1 (*continued*)

Gene name	MM or UB enrichment	Fold change	Reference	Gene name	MM or UB enrichment	Fold change	Reference
Hoxa11	MM	4.4	(Patterson and Potter, 2004)	Sema5b	UB	4.4	
Ebf2	MM	4.4		Gfra1	UB	4.4	(Enomoto et al., 1998)
Gfra3	MM	4.4		Hoxb7	UB	4.4	(Patterson and Potter, 2004)
Ccl19	MM	4.1		Dkk1	UB	4.4	
Tbx1	MM	3.9		Myb	UB	4.3	
Fgfr3	MM	3.8		En2	UB	4.2	
Gli1	MM	3.8		Lamc1	UB	4.1	(Virtanen et al., 1995)
Cxcl13	MM	3.7		Cyr61	UB	3.9	(Schmidt-Ott et al., 2005)
Slit3	MM	3.7	(Piper et al., 2000)	Mal	UB	3.8	
Ccl6	MM	3.7		Lhx8	UB	3.7	
Slit3	MM	3.7		Itga3	UB	3.7	
Hoxc9	MM	3.6	(Patterson and Potter, 2004)	Slit2	UB	3.6	(Grieshammer et al., 2004)
Pbx1	MM	3.6	(Schnabel et al., 2003)	Fzd4	UB	3.6	
Pbx3	MM	3.5		Sema6a	UB	3.6	
Sfrp1	MM	3.2	(Yoshino et al., 2001)	Cklfsf8	UB	3.5	
Eya2	MM	3.2		Cxcr4	UB	3.4	
Notch4	MM	3.1		Sema5a	UB	3.4	
Sfrp2	MM	3.1		Cited4	UB	3.3	
Hoxd11	MM	3.1	(Patterson et al., 2001)	Sema3d	UB	3.2	
Ccr1	MM	3.1		Sema3b	UB	3.1	

and real time PCR was generally excellent (CXCL12, 3.3 vs. 2.8, TGFbeta2, 3.6 vs. 3.3, pdgfrb, 2.1 vs. 1.5), although for two genes the real time PCR found a much greater fold change than the microarrays (Slit3, 2.3 vs. 7.8, Hoxa11antisense, −5 vs. −34). These results suggest that by using a combined 17 microarrays, including two different platforms and examining two closely related developmental stages, it was possible to discern a list of genes with genuine expression differences in wild type and Hoxa11/d11 mutant kidneys.

The microarray data called eight genes with greater than 3-fold change in expression in the mutants. These are quite interesting genes, (GATA6, TGFbeta2, chemokine ligand 12, angiotensin receptor like 1, cytochrome P450, cadherin5, Hoxa11 antisense and Lymphocyte antigen 6 complex), encoding a transcription factor, a growth factor, a chemokine, a receptor and a cell adhesion molecule. The bulk of genes differently expressed, however, showed lower fold changes, in the 1.5–3 range. We have previously shown that certain regions of the mutant kidneys, in particular the two poles, often show relatively normal development (Patterson et al., 2001). The more normal gene expression patterns in these

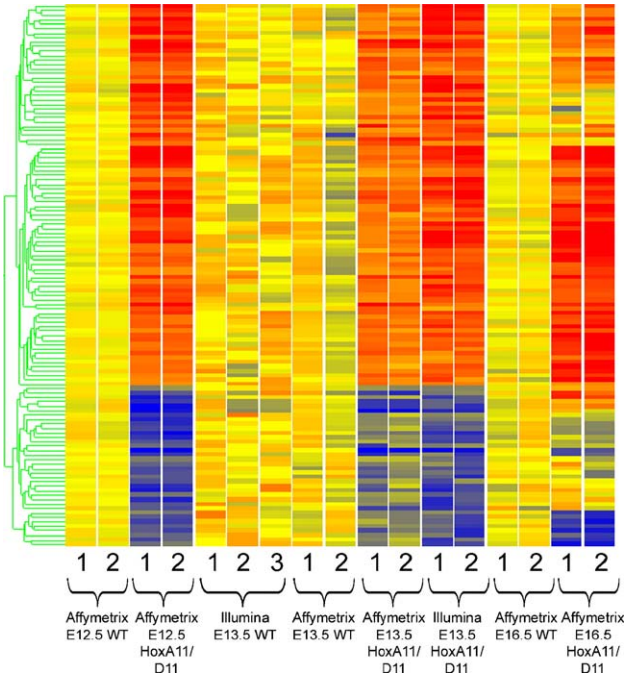

Fig. 4. Heat map showing 122 genes clustered according to differential expression in wild type and Hoxa11/Hoxd11 mutant kidneys. Expression levels were examined at E12.5, E13.5 and E16.5. Genes were selected by average fold change >1.5 at both E12.5 and E13.5, using both Affymetrix and Illumina microarray platforms (see text for details). All mutant expression levels were normalized to the corresponding microarray platform's wild type expression. Red indicates increased, blue indicates decreased and yellow shows unchanged expression. Most of the differences seen at E12.5 and E13.5 were also present at E16.5

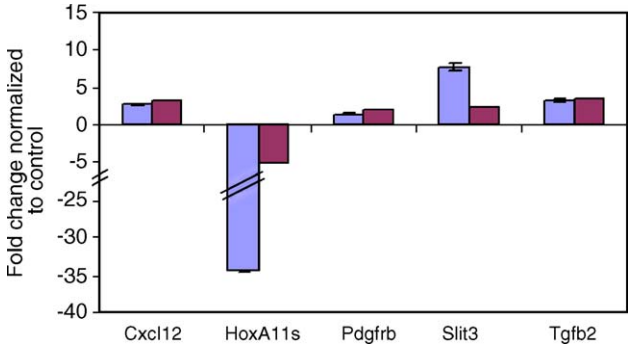

Fig. 5. QPCR validation of microarray predicted gene expression differences. Cxcl12, HoxA11s, Pdgfrb, Slit3, and Tgfb2 were examined. Separate E13.5 mutant and wild type kidney samples were assayed in sample groups of at least three. Graph shows mutant fold change normalized to wild type group according to QPCR (blue bars) or microarray data (red bars). The numbers agreed well, except for HoxAlls (HoxA11 antisense), and Slit3, where the QPCR called larger fold changes than the microarrays.

Table 2
122 genes differentially expressed between Hoxa11/d11 null and wild type whole kidneys consistently at both E12.5 and E13.5

Gene name	Fold change	Gene name	Fold change	Gene	Fold change
Gata6	3.9	BC039093	2	Tfip11	1.6
Tgfb2	3.6	Ptk2	2	Eps15-rs	1.6
Cxcl12	3.3	Sox18	2.1	Plcd1	1.5
Agtrl1	3.1	Eml1	2.1	AA408278	1.5
Cyp26b1	3.1	Igfbp4	2	Rbm4	−1.5
Cdh5	3.1	Col3a1	2	2010005O13Rik	−1.5
Gata6	3	Col18a1	2	Ptplb	−1.6
Sepn1	2.8	Col23a1	2	Rab25	−1.6
Rgs12	2.8	Fbn1	2	0610007A15Rik	−1.6
Tsc2	2.8	2310014H19Rik	2	Timm13a	−1.6
Smad6	2.8	6720469N11Rik	2	Hagh	−1.6
Ltbp1	2.7	Ube2r2	1.9	Ppie	−1.6
Pdgfrb	2.6	Cul7	1.9	Hmgb1	−1.6
9-Sep	2.6	Ldb1	1.9	2700085M18Rik	−1.6
2610001E17Rik	2.6	Col5a1	1.9	2310003L22Rik	−1.7
Agtrl1	2.5	BC025600	1.9	6330548G22Rik	−1.7
Fbn1	2.5	1110012D08Rik	1.9	Atp5h	−1.7
Vegfc	2.5	Sidt2	1.9	Hagh	−1.7
Col5a1	2.5	E130203B14Rik	1.9	Rcl1	−1.8
Sec31l1	2.5	Ephb4	1.9	Npm3	−1.8
Col4a2	2.4	Mast2	1.9	Gkap1	−1.8
Vars2	2.4	Lnk	1.9	Khdrbs1	−1.8
Sbk	2.4	1300018I05Rik	1.8	Hmgb1	−1.8
4933409N07Rik	2.4	Myo7a	1.8	1700021F05Rik	−1.8
Maml1	2.3	BC004012	1.8	2410019A14Rik	−1.9
Col23a1	2.3	1100001D10Rik	1.8	1700001E16Rik	−1.9
Mmp11	2.3	Igfbp4	1.8	Hnrpa3	−1.9
Slit3	2.3	Zbtb5	1.8	Psma7	−1.9
Col18a1	2.3	D10Ertd610e	1.7	Car4	−1.9
Foxd1	2.3	Plekhm1	1.7	Ggt1	−2
Sulf2	2.2	Ctxn	1.7	Drg1	−2
Emilin1	2.2	Thsd1	1.7	Hcngp	−2
Emilin1	2.2	BC033915	1.7	Hnrpdl	−2.1
AI450540	2.2	Lhfpl2	1.7	Pmvk	−2.1
Actr1a	2.2	Anxa6	1.7	Car4	−2.1
Robo4	2.2	Maml1	1.7	Hsd17b7	−2.2
Islr	2.1	Zdhhc7	1.6	Nudt5	−2.2
Bace1	2.1	Lhfpl2	1.6	Fkbp2	−2.4
4732495E13Rik	2.1	Inpp5e	1.6	Ly6a	−3.7
Pdgfrb	2.1	Nsg2	1.6	Hoxa11s	−5.1
6530411B15Rik	2	AI450540	1.6		

regions would dilute out gene expression differences present in the severely developmentally perturbed ventral–medial part of the mutant kidney. It is likely, therefore, that our results represent underestimates of the fold changes present in the most abnormal regions.

Comparison of wild type and Hoxa11/d11 mutant E11.5 MM

The E11.5 time point is of particular interest in the analysis of the Hoxa11/d11 mutants. Both Hoxa11 and Hoxd11 are expressed in the E11.5 MM, and at this early stage the MM appears histologically normal. Nevertheless it is functionally deficient. In some mutants with severe phenotypes we have observed that the UB forms, and penetrates the MM. However, instead of stopping and branching the UB simply grows right through the MM, exiting the other side (Patterson, unpublished observations). The Hoxa11/d11 genes clearly play an important role in communication between the early UB and MM.

To perform a global analysis of the altered gene expression pattern in the E11.5 MM we used a strategy similar to that described for the E12.5/E13.5 wild type-mutant comparison. To improve purity of starting material, we used laser capture microdissection to isolate MM from wild type and mutant E11.5 embryos. Following RNA purification and two round in vitro transcription target amplification, we used the Affymetrix MOE430 microarrays to determine gene expression levels. To achieve high throughput validation of the resulting gene list, we then repeated this process, using the Illumina platform, looking for genes consistently called differently expressed in wild type and mutant E11.5 MM by both systems. Each microarray used an independent biological sample (biological replicate). Again, a total of 17 microarrays were used for the comparison, in this case with 12 Affymetrix and 5 Illumina microarrays. The data were analyzed with GeneSpring 7.0, using similar parameters to those described for the E12.5/E13.5 data, except with a more stringent expression threshold cutoff. In this case we required a

minimum raw expression level of at least 600 in two samples, versus the cutoff of 400 used for the E12.5, E13.5 data. Genes with low expression levels give low signal to noise ratios and are a major source of artifacts. In both sets of comparisons, we eliminated the bulk of these false calls by setting stringent minimal expression requirements.

This analysis provided a list of 146 genes showing greater than 1.5-fold change in expression in the mutant E11.5 MM. The consistency of these expression differences across the seventeen samples, including both microarray platforms, is illustrated in the series graph of Fig. 6. The gene list, with observed fold changes, is provided in Table 3. We found six genes with greater than 3-fold change in expression. Iroquois 3 (Irx3), encoding a homeodomain transcription factor, was up-regulated 6-fold, and the EST A930038C07Rik was up-regulated 3.5-fold. Down-regulated genes included Meox2 (−3.4) also encoding a homeodomain protein, Hoxa11 antisense (−4.4), Prkcn (−4.5) encoding a protein kinase C, and Slc40a1 (−5.2, −6.1), encoding an iron transporter. In addition there are a number of interesting genes with smaller fold expression changes in the 1.5–3 range, some of which are discussed later.

Together, these extensive microarray studies of the altered gene expression patterns present in the Hoxa11/d11 mutant kidneys provide deeper insight in the normal functions of the Hox11 group of genes, as discussed further below.

Discussion

Microarrays provide a powerful technology for the analysis of both normal and mutant kidney development. The pioneering work of Stuart et al. (2001) used Affymetrix microarrays to examine normal rat kidney development, identifying several important functional groupings and thousands of specific genes not previously associated with kidney development. This work was subsequently extended to the developing mouse kidney (Schwab et al., 2003). Several recent reports have taken the microarray analysis of kidney development a step further, with Challen et al. (2004) using cDNA arrays to define the genes expressed specifically in the E10.5 uninduced MM, compared to more rostral uninduced intermediate mesoderm, in order to better define the nature of the early renal stem cell. Challen et al. (2005) also conducted an extensive cDNA microarray analysis of the gene expression profiles of total developing kidneys at multiple stages, as well as GFP sorted UB at E15.5. In another important study Schmidt-Ott et al. (2005) manually micro-dissected UB tips and mesenchyme from both mouse (E12.5) and rat (E13.5) and used Affymetrix microarrays to find differentially expressed genes. Of particular interest they identified the cytokine Clf-1 as a novel regulator secreted by the UB. In this report we extend this growing microarray database of normal kidney development by using the Affymetrix MOE430 generation microarray to determine gene expression profiles of total kidneys at multiple stages of development.

We also performed an extensive analysis of E11.5 MM and UB gene expression patterns, including laser capture microdissection to insure tissue purity, and using a total of eleven microarrays to provide great statistical power in the analysis. This resulted in a comprehensive definition of the gene expression states of these two critical early kidney components. We identified 1518 genes with over 3-fold divergent expression, including growth factors, cytokines, receptors, and transcription

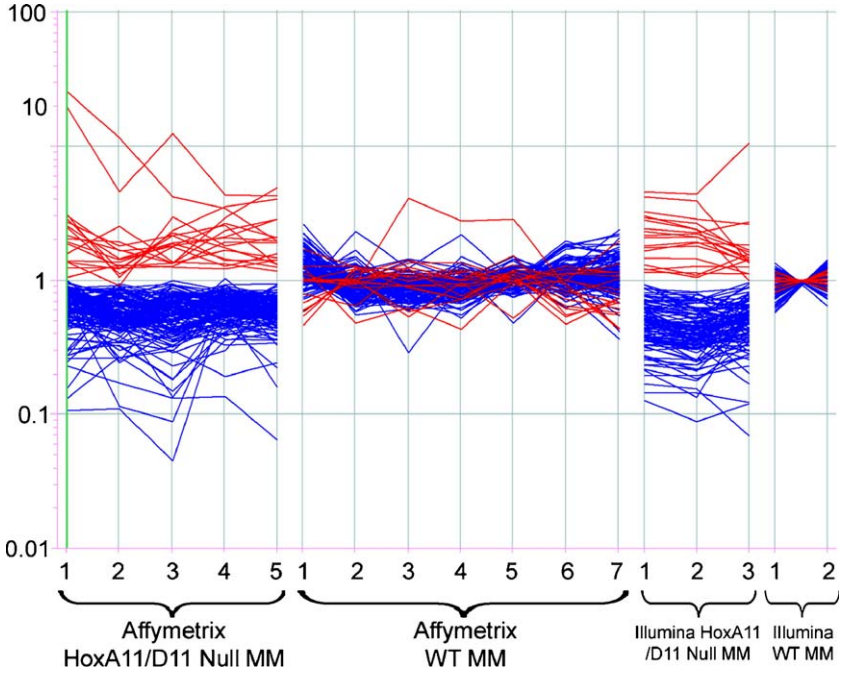

Fig. 6. Log series graph of 146 genes differentially expressed between HoxA11/D11 null and wild type E11.5 MM. This graph shows the consistent change in expression for these genes using both the Affymetrix and Illumina platforms. Genes were selected on statistical significance and an average fold change of >1.5 regardless of platform (see text for details). Gene in red are up-regulated and those in blue are down-regulated, as normalized to wild type.

Table 3
146 genes differentially expressed between HoxA11/D11 null and wild type E11.5 MM

Gene name	Fold change	Gene name	Fold change	Gene	Fold change
Irx3	6	Sall2	−1.6	Hus1	−1.8
A930038C07Rik	3.5	Sfrs1	−1.6	2700023B17Rik	−1.8
Hs3st3a1	2.7	Eif3s5	−1.6	Gtl6	−1.8
4930422J18Rik	2.4	Luc7l2	−1.6	Pfdn2	−1.8
1110055E19Rik	2.3	Yap1	−1.6	4432404J10Rik	−1.8
Slc6a8	2.2	Tardbp	−1.6	Pfn2	−1.8
Prcc	2	Arpp19	−1.6	Prkcn	−1.8
Elovl4	1.9	1110002B05Rik	−1.6	E230022H04Rik	−1.8
Ccnd1	1.9	Acaa1	−1.6	Fignl1	−1.8
Ltap	1.8	Zfp292	−1.6	Gltp	−1.9
Tiam1	1.8	Becn1	−1.6	Dhx15	−1.9
Tm4sf13	1.7	Tcte1l	−1.6	Trim25	−1.9
Epb4.1l4a	1.7	Dazap2	−1.6	Mtf2	−1.9
Cacna1h	1.7	Casp2	−1.6	Vps54	−1.9
Sfrs2	1.7	Topors	−1.6	Hnrpa1	−1.9
Tm4sf9	1.6	Gng10	−1.6	4833420G17Rik	−1.9
Dbn1	1.6	Zcchc6	−1.6	D11Ertd333e	−1.9
1100001I19Rik	1.6	Hoxa5	−1.6	Dhx15	−1.9
Ogt	−1.5	Acaa1	−1.6	Hoxd10	−2
AW549877	−1.5	Suhw3	−1.6	Kbtbd2	−2
D16Bwg1543e	−1.5	Tnrc6	−1.6	Rassf1	−2
Pole4	−1.5	AW539964	−1.6	Thsd2	−2
2700029M09Rik	−1.5	Purb	−1.6	Hnrpdl	−2
Pygb	−1.5	Tnrc6	−1.6	BC019806	−2
Sh3bgrl	−1.5	Eif4a2	−1.6	Foxc2	−2
5730526G10Rik	−1.5	Mrg1	−1.6	Hnrpdl	−2.1
1110028E10Rik	−1.5	Rps6	−1.6	Rassf1	−2.1
Zhx1	−1.5	Prkwnk1	−1.7	Eml4	−2.2
1810043J12Rik	−1.5	Srp14	−1.7	1110021E09Rik	−2.2
Mcm4	−1.5	Msh6	−1.7	Cul1	−2.2
Mrps33	−1.5	D11Ertd333e	−1.7	Pja2	−2.2
Arf3	−1.5	Rab24	−1.7	2810485I05Rik	−2.3
5930412E23Rik	−1.5	6330412F12Rik	−1.7	8430438D04Rik	−2.4
2700023B17Rik	−1.5	Qrsl1	−1.7	Kbtbd2	−2.4
1110003E01Rik	−1.5	Ncoa6ip	−1.7	Cox7a2l	−2.4
Gtl6	−1.5	6330578E17Rik	−1.7	Cox7a2l	−2.4
Tbk1	−1.5	Mrg1	−1.8	Cno	−2.5
5930412E23Rik	−1.5	Mrpl50	−1.8	Tpm2	−2.5
Fgfr1op	−1.6	Zfp68	−1.8	Shoc2	−2.5
Rhobtb3	−1.6	Tubb6	−1.8	Wsb1	−2.6
Pldn	−1.6	Ibtk	−1.8	Tpm2	−2.7
Pafah1b1	−1.6	Wasl	−1.8	Tpm2	−2.7
Gas5	−1.6	Hus1	−1.8	Meox2	−3.4
Tardbp	−1.6	2700023B17Rik	−1.8	Hoxa11s	−4.4
4121402D02Rik	−1.6	Gtl6	−1.8	Prkcn	−4.5
Ets2	−1.6	Ibtk	−1.8	Slc40a1	−5.2
2610208E05Rik	−1.6	Wasl	−1.8	Slc40a1	−6.1
1110004P21Rik	−1.6				

factors that presumably drive the reciprocal inductive interactions and differential development of these two tissues.

This set of data for normal kidney development then provides the foundation for the microarray analysis of kidney mutant phenotypes. In this study, we focused on the analysis of the Hoxa11/Hoxd11 double homozygous mutant kidneys at early stages of development. At E11.5, the invading UB has branched once, forming a T-shaped structure, and the MM has not yet formed even the earliest epithelial nephron precursor, the renal vesicle. It is important to emphasize that in this study we used laser capture microdissection to purify wild type and mutant E11.5 MM for microarray analysis. A little later, at E12.5 and E13.5, the UB has undergone multiple branches and early nephrogenesis is underway. By looking at these early times, we increased the likelihood of finding initiating events in the Hoxa11/Hoxd11 mutant disturbed genetic program of kidney development. These early changes in gene expression in the mutant can then presumably give rise to further downstream cascade effects at later times, which might also be interesting, but could be secondary to dramatic changes in cell differentiation and/or relative abundances of different cell type populations.

We found that the subtle changes in gene expression present in the mutants at early time points were difficult to tease out

with microarrays. Indeed, at each developmental stage analyzed, E11.5, and the combined E12.5/E13.5, we found it necessary to use 17 microarrays. Of particular interest, we found that the use of two independent microarray platforms, Affymetrix and Illumina, coupled with independent biological samples, greatly strengthened the study.

A key bottleneck in microarray studies is the validation process. After the microarray data is generated and analyzed a gene list is made. There must, however, be supporting evidence indicating that the gene list is authentic. In this study we found that in our initial comparisons of early wild type and mutant embryonic kidneys, even when using as many as eight Affymetrix microarrays, over half of the genes called differently expressed by microarray were failing to validate by real time PCR. Indeed, we were unable to set a stringency of analysis that clearly distinguished the genes that validated with real time PCR. The use of an additional microarray platform, however, with independent biological replicates, appeared to provide an effective high throughput validation. Genes called differently expressed by both systems consistently validated by real time PCR. This might be an extremely useful general validation strategy, offering a rapid method for separating true differences from artifacts. Instead of checking for genuine gene expression differences one at a time by real time PCR, one uses a distinct microarray system with new biological samples to confirm changes en masse.

It is interesting that for the wild type-Hoxa11/d11 mutant comparison at both E11.5 and the combined E12.5/E13.5 stages we observed relatively few genes with greater than 3-fold expression change. It was reassuring to find a Hoxa11 transcript (Hoxa11 antisense) common to both lists. It was somewhat surprising, however, to find that the two lists of differently expressed genes had very little else in common. Our previous molecular marker studies of these mutant kidneys indicated that the Hox11 genes function in multiple processes at several stages of kidney development, and these distinct gene lists could reflect timing specific variations in function. The Hox11 genes could be driving distinct processes at these two stages. It is also possible that some of the observed differences at E12.5/13.5 could be the result of downstream effects of the earlier changes.

The gene showing the largest fold change in the Hoxa11/d11 mutant kidney at E11.5 was the homeobox gene Irx3, which was up-regulated 6-fold. It is quite interesting that earlier experiments have shown that Irx3 is also a downstream target of both Hoxa9 and Hoxa10 in hematopoietic cells (Ferrell et al., 2005). The Hox9, 10 and 11 paralogous groups are all very closely related Abd-b type Hox genes, and it is not surprising to see overlap in their downstream targets. In yet another study, looking at development of the hindbrain, it was shown that over expression of Hoxa3, a more distant relative of the Hox11 genes, caused repression of Irx3 transcription (Guidato et al., 2003). These previous connections between Hox genes and Irx3 support the conclusion that Irx3 is a true downstream effector of Hoxa11/d11 in the developing kidney. It is also interesting that these different Hox genes would share this same target in these different developing systems, although again this is perhaps not surprising in light of the similarities of their DNA binding homeodomains. As multiple targets for multiple Hox genes are unveiled we gain a deeper understanding of Hox functional relationships.

The functions of Irx3 in kidney development remain uncertain. Irx3 has been shown to be capable of regulating competence to respond to hedgehog signaling in the nervous system (Kiecker and Lumsden, 2004). It has also been shown that Irx3 expression can be directed by Wnt signaling in the nervous system (Braun et al., 2003). These observations suggest a possible connection between Irx3 and growth factor signaling in the developing kidney. It has also been previously shown that Irx3 is expressed in the normal developing kidney, but primarily in a more mature structure, the forming glomerulus (Houweling et al., 2001).

The gene with the second greatest fold change in the Hoxa11/d11 mutant kidneys at E11.5 was Slc40a1, an iron exporter also known as Ferroportin1. On two separate probe sets this gene showed down-regulation of −5.2 and −6.1. This is an especially intriguing observation because of the known importance of iron in kidney development. When growing kidneys in organ culture it is necessary to add Fe^{3+}-transferrin to minimal essential media to promote robust branching morphogenesis of the UB and nephrogenesis of the MM (Landschulz and Ekblom, 1985). Furthermore, another iron transporter, lipocalin, also known as NGAL, has been shown to be an important inducer of nephrogenesis secreted by the UB (Yang et al., 2003). This established connection between iron levels and nephrogenesis, and our observation that the expression of the Ferroportin1 gene is significantly down-regulated in the mutants, suggests that one molecular mechanism of function of Hoxa11 and Hoxd11 in kidney development might be through the regulation of intracellular iron levels.

Two other genes showed a more than 3-fold down-regulation in the E11.5 mutant MM. Prkcn, a member of the protein kinase C family, showed a 4.5-fold reduction in mutants. It has been previously shown that a number of PKC inhibitors disturb nephron formation and inhibit growth of kidneys in organ culture (Yang et al., 2003). It is interesting that the inhibition of PKC gives a phenotype resembling that produced by Hoxa11/d11 mutation.

The homeobox gene Meox2 (also named Gax) was down-regulated 3.4-fold in the E11.5 mutant kidney. Previous studies have demonstrated that over-expression of Meox2 can reduce cell proliferation rates (Fisher et al., 1997; Smith et al., 1997). This seems somewhat paradoxical, since the mutant kidney shows reduced Meox2 expression, and reduced size. The Meox2 gene has also been connected to regulation of cell migration and integrin expression (Perlman et al., 1999).

Our E12.5/13.5 data provided further evidence that Meox2 is a genuine downstream target of Hoxa11/Hoxd11 in kidney development. The Affymetrix microarray data also found a significant decrease in Meox2 expression in the mutants at this later stage (−3.5-fold change). Real time PCR validation confirmed this difference at E13.5 (−5.7-fold change, data not shown). The Illumina microarrays also detected an expression change in this gene (−3.0-fold), but the observed P value of 0.11 did not make the <0.05 cutoff, so Meox2 was not

included in our final list of genes called differently expressed at this later stage.

Several other genes of interest showed altered expression in the E11.5 mutant kidneys, including tropomyosin 2 beta (−2.7-fold, −2.7, and −2.5 on three separate probe sets), an important component of the cytoskeleton, Wsb1 (−2.6-fold), a hedgehog inducible ubiquitin ligase (Dentice et al., 2005), and shoc2 (−2.5-fold), a gene involved in fibroblast growth factor receptor signaling (Selfors et al., 1998). Other genes that showed lower fold changes included Zhx1 (−1.5-fold) a zinc finger-homeobox gene that is induced by cytokines (Shou et al., 2004), Sall2 (−1.6), Foxc2 (−2.0), which has been shown to have an important role in kidney development (Kume et al., 2000a), Rab24 (−1.7), a member of the Ras oncogene family, and Rassf1 (−2.0, −2.1) a Ras associated domain family member.

At E12.5/13.5 the gene showing the greatest up-regulation encodes the transcription factor Gata6 (3.6- and 3.0-fold change on two separate probe sets). This is particularly interesting because over expression of Gata6 has been previously shown to cause growth arrest, in both vascular myocytes and glomerular mesangial cells (Nagata et al., 2000), correlating nicely with the observed reduced size of the Hoxa11/d11 mutant kidney.

Interestingly, four members of the TGF-beta pathway were also up-regulated at E12.5/13.5, including Tgfb2 (3.6-fold), Smad6 (2.8), Ltbp1 (2.7), and fibrillin (2.5, 2.0). Several previous studies have shown the importance of TGF signaling in kidney development. Tgfb2 has been shown to be expressed in both the MM and UB, and can induce nephrogenesis when added to MM culture along with FGF2 (Plisov et al., 2001). The Tgfb2 knockout mouse shows a renal agenesis phenotype, with incomplete penetrance (Sanford et al., 1997). A conditional MM knockout of Smad4, the downstream activator of TGF-beta signaling, results in abnormal nephrogenesis (Oxburgh et al., 2004). Smad6, an inhibitory Smad, interacts downstream of TGF-beta signals to negatively regulate transcription activation, and interestingly is specifically expressed in the nephrogenic mesenchyme and UB tips of the developing kidney (Vrljicak et al., 2004). The Fibrillin1 and Ltbp1 genes encode structurally related proteins. TGF-beta is secreted as a latent complex that includes the latent TGF-beta binding protein (Ltbp1) (Annes et al., 2003). The Fibrillin1 protein is a matrix component of the extracellular microfibrils and plays an important role in TGF-beta activation (Neptune et al., 2003). This observed dysregulation of expression of Tgfb2, Smad6, Ltbp1 and fibrillin1 suggests an important role for Hox11 genes in the control of TGF-beta signaling in the developing kidney.

Other notable genes up-regulated in the HoxA11/D11 mutant E12.5/E13.5 kidneys include, Cxcl12 (3.3-fold), Ldb1 (1.9), Slit3 (2.3), and Robo4 (2.2). Cxcl12 is a small, c–x–c motif chemokine that is expressed in comma and s-shaped bodies during nephrogenesis and within the mesangium of the maturing glomeruli (Grone et al., 2002). Lbd1 is a cofactor that can interact with many transcription factors, including LIM-homeodomain proteins such Lhx1, which is required for both normal UB branching morphogenesis and developmental progression of the renal vesicle during nephrogenesis (Kobayashi et al., 2005). Lbd1 can increase or decrease transcription factor activity, with correct Lbd1-LIMHD stoichiometry essential for normal development (Neptune et al., 2003). Overexpression of Ldb1 has been associated with a block of differentiation in both immature erythroid cells and mammary epithelial cells (Visvader et al., 1997, 2001). Slit2 and its receptor Robo2 have been shown to restrict GDNF expression in the intermediate mesoderm thereby restricting the site of the UB formation (Grieshammer et al., 2004). Slit3 and/or Robo4 may have similar roles in repression of GDNF expression. The microarray observed over expression of Slit3 and Robo4 would then be predicted to result in reduced levels of GDNF, and this was indeed found. The level of down-regulation was, however, only 1.3-fold, and therefore not sufficient to make the 1.5-fold cutoff used to make the list of differently expressed genes. These results suggest, but do not prove, that the previously observed loss of GDNF expression in Hox11 triple mutants (Hoxa11, Hoxc11, Hoxd11) (Wellik et al., 2002) might be mediated through increased Slit–Robo expression.

In conclusion, the microarray analysis of a mutant phenotype can be challenging, yet highly rewarding. By examining the early stages of a developmental abnormality, one defines the initiating events, but the differences present between wild type and mutant at this point might be subtle, with many genes showing small changes in expression. In order to obtain convincing results, we found it necessary to use 17 microarrays to compare E12.5/E13.5 wild type and mutant, and then another 17 microarrays to compare E11.5. The initial analysis was performed with Affymetrix microarrays. We found that the use of a second microarray platform, Illumina, with independent biological samples, provided a high throughput validation that effectively separated genuine differences from artifacts.

The results of this study identify multiple Hox11 effectors in kidney development. Many of the genes with altered expression make sense. The gene with the greatest up-regulation at E11.5, Irx3, has been previously identified as a downstream target of three other Hox genes. In addition, the up-regulation of Gata6, the perturbation of iron transport, PKC levels, TGF-beta signaling, Lbd1, Slit and Robo all fit with the observed kidney phenotype of reduced size, reduced branching morphogenesis and altered MM–UB interactions. As more microarray studies are performed on more Hox mutants, in both kidney and other tissues, we will gain deeper insight into the molecular mechanisms of Hox function and the extent of Hox functional overlap.

Acknowledgments

We thank Michael Bennett for help with embryo block preparation, discussions regarding RT-PCR validations, and careful reading of the manuscript. We thank Kristen Saletel and Shawn Smith for generation of microarray data. This work was supported by NIH grant 1RO1DK61916.

Appendix A. Supplementary data

Supplementary data associated with this article can be found in the online version at doi:10.1016/j.ydbio.2006.02.023.

References

Annes, J.P., Munger, J.S., Rifkin, D.B., 2003. Making sense of latent TGFbeta activation. J. Cell Sci. 116, 217–224.

Basson, M.A., Akbulut, S., Watson-Johnson, J., Simon, R., Carroll, T.J., Shakya, R., Gross, I., Martin, G.R., Lufkin, T., McMahon, A.P., Wilson, P.D., Costantini, F.D., Mason, I.J., Licht, J.D., 2005. Sprouty1 is a critical regulator of GDNF/RET-mediated kidney induction. Dev. Cell 8, 229–239.

Bolstad, B.M., Irizarry, R.A., Astrand, M., Speed, T.P., 2003. A comparison of normalization methods for high density oligonucleotide array data based on variance and bias. Bioinformatics 19, 185–193.

Bouchard, M., 2004. Transcriptional control of kidney development. Differentiation 72, 295–306.

Brandenberger, R., Schmidt, A., Linton, J., Wang, D., Backus, C., Denda, S., Muller, U., Reichardt, L.F., 2001. Identification and characterization of a novel extracellular matrix protein nephronectin that is associated with integrin alpha8beta1 in the embryonic kidney. J. Cell Biol. 154, 447–458.

Braun, M.M., Etheridge, A., Bernard, A., Robertson, C.P., Roelink, H., 2003. Wnt signaling is required at distinct stages of development for the induction of the posterior forebrain. Development 130, 5579–5587.

Brunskill, E.W., Witte, D.P., Yutzey, K.E., Potter, S.S., 2001. Novel cell lines promote the discovery of genes involved in early heart development. Dev. Biol. 235, 507–520.

Candia, A.F., Hu, J., Crosby, J., Lalley, P.A., Noden, D., Nadeau, J.H., Wright, C.V., 1992. Mox-1 and Mox-2 define a novel homeobox gene subfamily and are differentially expressed during early mesodermal patterning in mouse embryos. Development 116, 1123–1136.

Carroll, T.J., Park, J.S., Hayashi, S., Majumdar, A., McMahon, A.P., 2005. Wnt9b plays a central role in the regulation of mesenchymal to epithelial transitions underlying organogenesis of the Mammalian urogenital system. Dev. Cell 9, 283–292.

Challen, G.A., Martinez, G., Davis, M.J., Taylor, D.F., Crowe, M., Teasdale, R.D., Grimmond, S.M., Little, M.H., 2004. Identifying the molecular phenotype of renal progenitor cells. J. Am. Soc. Nephrol. 15, 2344–2357.

Challen, G., Gardiner, B., Caruana, G., Kostoulias, X., Martinez, G., Crowe, M., Taylor, D.F., Bertram, J., Little, M., Grimmond, S.M., 2005. Temporal and spatial transcriptional programs in murine kidney development. Physiol. Genomics 23, 159–171.

Cho, E.A., Patterson, L.T., Brookhiser, W.T., Mah, S., Kintner, C., Dressler, G.R., 1998. Differential expression and function of cadherin-6 during renal epithelium development. Development 125, 803–812.

Davies, J.A., Bard, J.B., 1998. The development of the kidney. Curr. Top. Dev. Biol. 39, 245–301.

Davis, A.P., Witte, D.P., Hsieh-Li, H.M., Potter, S.S., Capecchi, M.R., 1995. Absence of radius and ulna in mice lacking hoxa-11 and hoxd-11. Nature 375, 791–795.

Dentice, M., Bandyopadhyay, A., Gereben, B., Callebaut, I., Christoffolete, M.A., Kim, B.W., Nissim, S., Mornon, J.P., Zavacki, A.M., Zeold, A., Capelo, L.P., Curcio-Morelli, C., Ribeiro, R., Harney, J.W., Tabin, C.J., Bianco, A.C., 2005. The Hedgehog-inducible ubiquitin ligase subunit WSB-1 modulates thyroid hormone activation and PTHrP secretion in the developing growth plate. Nat. Cell Biol. 7, 698–705.

Durbec, P., Marcos-Gutierrez, C.V., Kilkenny, C., Grigoriou, M., Wartiowaara, K., Suvanto, P., Smith, D., Ponder, B., Costantini, F., Saarma, M., et al., 1996. GDNF signalling through the Ret receptor tyrosine kinase. Nature 381, 789–793.

Enomoto, H., Araki, T., Jackman, A., Heuckeroth, R.O., Snider, W.D., Johnson Jr., E.M., Milbrandt, J., 1998. GFR alpha1-deficient mice have deficits in the enteric nervous system and kidneys. Neuron 21, 317–324.

Fan, Q.W., Kadomatsu, K., Uchimura, K., Muramatsu, T., 1998. Embigin/basigin subgroup of the immunoglobulin superfamily: different modes of expression during mouse embryogenesis and correlated expression with carbohydrate antigenic markers. Dev. Growth Differ. 40, 277–286.

Ferrell, C.M., Dorsam, S.T., Ohta, H., Humphries, R.K., Derynck, M.K., Haqq, C., Largman, C., Lawrence, H.J., 2005. Activation of stem-cell specific genes by HOXA9 and HOXA10 homeodomain proteins in CD34+ human cord blood cells. Stem Cells 23, 644–655.

Fisher, S.A., Siwik, E., Branellec, D., Walsh, K., Watanabe, M., 1997. Forced expression of the homeodomain protein Gax inhibits cardiomyocyte proliferation and perturbs heart morphogenesis. Development 124, 4405–4413.

Grieshammer, U., Le, M., Plump, A.S., Wang, F., Tessier-Lavigne, M., Martin, G.R., 2004. SLIT2-mediated ROBO2 signaling restricts kidney induction to a single site. Dev. Cell 6, 709–717.

Grone, H.J., Cohen, C.D., Grone, E., Schmidt, C., Kretzler, M., Schlondorff, D., Nelson, P.J., 2002. Spatial and temporally restricted expression of chemokines and chemokine receptors in the developing human kidney. J. Am. Soc. Nephrol. 13, 957–967.

Guidato, S., Prin, F., Guthrie, S., 2003. Somatic motoneurone specification in the hindbrain: the influence of somite-derived signals, retinoic acid and Hoxa3. Development 130, 2981–2996.

Hatini, V., Huh, S.O., Herzlinger, D., Soares, V.C., Lai, E., 1996. Essential role of stromal mesenchyme in kidney morphogenesis revealed by targeted disruption of Winged Helix transcription factor BF-2. Genes Dev. 10, 1467–1478.

Houweling, A.C., Dildrop, R., Peters, T., Mummenhoff, J., Moorman, A.F., Ruther, U., Christoffels, V.M., 2001. Gene and cluster-specific expression of the Iroquois family members during mouse development. Mech. Dev. 107, 169–174.

Hsieh-Li, H.M., Witte, D.P., Weinstein, M., Branford, W., Li, H., Small, K., Potter, S.S., 1995. Hoxa 11 structure, extensive antisense transcription, and function in male and female fertility. Development 121, 1373–1385.

Itaranta, P., Lin, Y., Perasaari, J., Roel, G., Destree, O., Vainio, S., 2002. Wnt-6 is expressed in the ureter bud and induces kidney tubule development in vitro. Genesis 32, 259–268.

Kalatzis, V., Sahly, I., El-Amraoui, A., Petit, C., 1998. Eya1 expression in the developing ear and kidney: towards the understanding of the pathogenesis of Branchio-Oto-Renal (BOR) syndrome. Dev. Dyn. 213, 486–499.

Kiecker, C., Lumsden, A., 2004. Hedgehog signaling from the ZLI regulates diencephalic regional identity. Nat. Neurosci. 7, 1242–1249.

Kispert, A., Vainio, S., McMahon, A.P., 1998. Wnt-4 is a mesenchymal signal for epithelial transformation of metanephric mesenchyme in the developing kidney. Development 125, 4225–4234.

Klein, G., Langegger, M., Goridis, C., Ekblom, P., 1988. Neural cell adhesion molecules during embryonic induction and development of the kidney. Development 102, 749–761.

Kobayashi, A., Kwan, K.M., Carroll, T.J., McMahon, A.P., Mendelsohn, C.L., Behringer, R.R., 2005. Distinct and sequential tissue-specific activities of the LIM-class homeobox gene Lim1 for tubular morphogenesis during kidney development. Development 132, 2809–2823.

Kreidberg, J.A., Sariola, H., Loring, J.M., Maeda, M., Pelletier, J., Housman, D., Jaenisch, R., 1993. WT-1 is required for early kidney development. Cell 74, 679–691.

Kume, T., Deng, K., Hogan, B.L., 2000a. Minimal phenotype of mice homozygous for a null mutation in the forkhead/winged helix gene, Mf2. Mol. Cell. Biol. 20, 1419–1425.

Kume, T., Deng, K., Hogan, B.L., 2000b. Murine forkhead/winged helix genes Foxc1 (Mf1) and Foxc2 (Mfh1) are required for the early organogenesis of the kidney and urinary tract. Development 127, 1387–1395.

Labastie, M.C., Catala, M., Gregoire, J.M., Peault, B., 1995. The GATA-3 gene is expressed during human kidney embryogenesis. Kidney Int. 47, 1597–1603.

Landschulz, W., Ekblom, P., 1985. Iron delivery during proliferation and differentiation of kidney tubules. J. Biol. Chem. 260, 15580–15584.

Lim, K.C., Lakshmanan, G., Crawford, S.E., Gu, Y., Grosveld, F., Engel, J.D., 2000. Gata3 loss leads to embryonic lethality due to noradrenaline deficiency of the sympathetic nervous system. Nat. Genet. 25, 209–2012.

Livak, K.J., Schmittgen, T.D., 2001. Analysis of relative gene expression data using real-time quantitative PCR and the 2(-Delta Delta C(T)) method. Methods 25, 402–408.

Loughna, S., Hardman, P., Landels, E., Jussila, L., Alitalo, K., Woolf, A.S.,

1997. A molecular and genetic analysis of renalglomerular capillary development. Angiogenesis 1, 84–101.

Majumdar, A., Vainio, S., Kispert, A., McMahon, J., McMahon, A.P., 2003. Wnt11 and Ret/Gdnf pathways cooperate in regulating ureteric branching during metanephric kidney development. Development 130, 3175–3185.

Miyamoto, N., Yoshida, M., Kuratani, S., Matsuo, I., Aizawa, S., 1997. Defects of urogenital development in mice lacking Emx2. Development 124, 1653–1664.

Miyazaki, Y., Oshima, K., Fogo, A., Hogan, B.L., Ichikawa, I., 2000. Bone morphogenetic protein 4 regulates the budding site and elongation of the mouse ureter. J. Clin. Invest. 105, 863–873.

Moore, M.W., Klein, R.D., Farinas, I., Sauer, H., Armanini, M., Phillips, H., Reichardt, L.F., Ryan, A.M., Carver-Moore, K., Rosenthal, A., 1996. Renal and neuronal abnormalities in mice lacking GDNF. Nature 382, 76–79.

Muller, U., Wang, D., Denda, S., Meneses, J.J., Pedersen, R.A., Reichardt, L.F., 1997. Integrin alpha8beta1 is critically important for epithelial–mesenchymal interactions during kidney morphogenesis. Cell 88, 603–613.

Nagata, D., Suzuki, E., Nishimatsu, H., Yoshizumi, M., Mano, T., Walsh, K., Sata, M., Kakoki, M., Goto, A., Omata, M., Hirata, Y., 2000. Cyclin A downregulation and p21(cip1) upregulation correlate with GATA-6-induced growth arrest in glomerular mesangial cells. Circ. Res. 87, 699–704.

Nagy, A., 2003. Manipulating the Mouse Embryo: A Laboratory Manual. Cold Spring Harbor Laboratory Press, Cold Spring Harbor, NY.

Neptune, E.R., Frischmeyer, P.A., Arking, D.E., Myers, L., Bunton, T.E., Gayraud, B., Ramirez, F., Sakai, L.Y., Dietz, H.C., 2003. Dysregulation of TGF-beta activation contributes to pathogenesis in Marfan syndrome. Nat. Genet. 33, 407–411.

Nishinakamura, R., Matsumoto, Y., Nakao, K., Nakamura, K., Sato, A., Copeland, N.G., Gilbert, D.J., Jenkins, N.A., Scully, S., Lacey, D.L., Katsuki, M., Asashima, M., Yokota, T., 2001. Murine homolog of SALL1 is essential for ureteric bud invasion in kidney development. Development 128, 3105–3115.

Oliver, G., Wehr, R., Jenkins, N.A., Copeland, N.G., Cheyette, B.N., Hartenstein, V., Zipursky, S.L., Gruss, P., 1995. Homeobox genes and connective tissue patterning. Development 121, 693–705.

Oxburgh, L., Chu, G.C., Michael, S.K., Robertson, E.J., 2004. TGFbeta superfamily signals are required for morphogenesis of the kidney mesenchyme progenitor population. Development 131, 4593–4605.

Patterson, L.T., Potter, S.S., 2004. Atlas of Hox gene expression in the developing kidney. Dev. Dyn. 229, 771–779.

Patterson, L.T., Pembaur, M., Potter, S.S., 2001. Hoxa11 and Hoxd11 regulate branching morphogenesis of the ureteric bud in the developing kidney. Development 128, 2153–2161.

Perlman, H., Luo, Z., Krasinski, K., Le Roux, A., Mahfoudi, A., Smith, R.C., Branellec, D., Walsh, K., 1999. Adenovirus-mediated delivery of the Gax transcription factor to rat carotid arteries inhibits smooth muscle proliferation and induces apoptosis. Gene Ther. 6, 758–763.

Pichel, J.G., Shen, L., Sheng, H.Z., Granholm, A.C., Drago, J., Grinberg, A., Lee, E.J., Huang, S.P., Saarma, M., Hoffer, B.J., Sariola, H., Westphal, H., 1996. Defects in enteric innervation and kidney development in mice lacking GDNF. Nature 382, 73–76.

Piper, M., Georgas, K., Yamada, T., Little, M., 2000. Expression of the vertebrate Slit gene family and their putative receptors, the Robo genes, in the developing murine kidney. Mech. Dev. 94, 213–217.

Plisov, S.Y., Yoshino, K., Dove, L.F., Higinbotham, K.G., Rubin, J.S., Perantoni, A.O., 2001. TGF beta 2, LIF and FGF2 cooperate to induce nephrogenesis. Development 128, 1045–1057.

Quaggin, S.E., Schwartz, L., Cui, S., Igarashi, P., Deimling, J., Post, M., Rossant, J., 1999. The basic-helix–loop–helix protein pod1 is critically important for kidney and lung organogenesis. Development 126, 5771–5783.

Rozen, S., Skaletsky, H., 2000. Primer3 on the WWW for general users and for biologist programmers. Methods Mol. Biol. 132, 365–386.

Ryan, G., Steele-Perkins, V., Morris, J.F., Rauscher III, F.J., Dressler, G.R., 1995. Repression of Pax-2 by WT1 during normal kidney development. Development 121, 867–875.

Sanchez, M.P., Silos-Santiago, I., Frisen, J., He, B., Lira, S.A., Barbacid, M., 1996. Renal agenesis and the absence of enteric neurons in mice lacking GDNF. Nature 382, 70–73.

Sanford, L.P., Ormsby, I., Gittenberger-de Groot, A.C., Sariola, H., Friedman, R., Boivin, G.P., Cardell, E.L., Doetschman, T., 1997. TGFbeta2 knockout mice have multiple developmental defects that are non-overlapping with other TGFbeta knockout phenotypes. Development 124, 2659–2670.

Saxen, L., Lehtonen, E., 1987. Embryonic kidney in organ culture. Differentiation 36, 2–11.

Schmidt-Ott, K.M., Yang, J., Chen, X., Wang, H., Paragas, N., Mori, K., Li, J.Y., Lu, B., Costantini, F., Schiffer, M., Bottinger, E., Barasch, J., 2005. Novel regulators of kidney development from the tips of the ureteric bud. J. Am. Soc. Nephrol. 16, 1993–2002.

Schnabel, C.A., Godin, R.E., Cleary, M.L., 2003. Pbx1 regulates nephrogenesis and ureteric branching in the developing kidney. Dev. Biol. 254, 262–276.

Schuchardt, A., D'Agati, V., Larsson-Blomberg, L., Costantini, F., Pachnis, V., 1994. Defects in the kidney and enteric nervous system of mice lacking the tyrosine kinase receptor Ret. Nature 367, 380–383.

Schwab, K., Patterson, L.T., Aronow, B.J., Luckas, R., Liang, H.C., Potter, S.S., 2003. A catalogue of gene expression in the developing kidney. Kidney Int. 64, 1588–1604.

Seifert, R.A., Alpers, C.E., Bowen-Pope, D.F., 1998. Expression of platelet-derived growth factor and its receptors in the developing and adult mouse kidney. Kidney Int. 54, 731–746.

Selfors, L.M., Schutzman, J.L., Borland, C.Z., Stern, M.J., 1998. soc-2 encodes a leucine-rich repeat protein implicated in fibroblast growth factor receptor signaling. Proc. Natl. Acad. Sci. U. S. A. 95, 6903–6908.

Shou, Z., Yamada, K., Kawata, H., Yokoyama, O., Miyamoto, K., 2004. A mechanism of induction of the mouse zinc-fingers and homeoboxes 1 (ZHX1) gene expression by interleukin-2. Biochem. Biophys. Res. Commun. 314, 885–890.

Small, K.M., Potter, S.S., 1993. Homeotic transformations and limb defects in Hox A11 mutant mice. Genes Dev. 7, 2318–2328.

Smith, R.C., Branellec, D., Gorski, D.H., Guo, K., Perlman, H., Dedieu, J.F., Pastore, C., Mahfoudi, A., Denefle, P., Isner, J.M., Walsh, K., 1997. p21CIP1-mediated inhibition of cell proliferation by overexpression of the gax homeodomain gene. Genes Dev. 11, 1674–1689.

Stark, K.L., McMahon, J.A., McMahon, A.P., 1991. FGFR-4, a new member of the fibroblast growth factor receptor family, expressed in the definitive endoderm and skeletal muscle lineages of the mouse. Development 113, 641–651.

Stark, K., Vainio, S., Vassileva, G., McMahon, A.P., 1994. Epithelial transformation of metanephric mesenchyme in the developing kidney regulated by Wnt-4. Nature 372, 679–683.

Stuart, R.O., Bush, K.T., Nigam, S.K., 2001. Changes in global gene expression patterns during development and maturation of the rat kidney. Proc. Natl. Acad. Sci. U. S. A. 98, 5649–5654.

Tessarollo, L., Nagarajan, L., Parada, L.F., 1992. c-ros: the vertebrate homolog of the sevenless tyrosine kinase receptor is tightly regulated during organogenesis in mouse embryonic development. Development 115, 11–20.

Virtanen, I., Laitinen, L., Korhonen, M., 1995. Differential expression of laminin polypeptides in developing and adult human kidney. J. Histochem. Cytochem. 43, 621–628.

Visvader, J.E., Mao, X., Fujiwara, Y., Hahm, K., Orkin, S.H., 1997. The LIM-domain binding protein Ldb1 and its partner LMO2 act as negative regulators of erythroid differentiation. Proc. Natl. Acad. Sci. U. S. A. 94, 13707–13712.

Visvader, J.E., Venter, D., Hahm, K., Santamaria, M., Sum, E.Y., O'Reilly, L., White, D., Williams, R., Armes, J., Lindeman, G.J., 2001. The LIM domain gene LMO4 inhibits differentiation of mammary epithelial cells in vitro and is overexpressed in breast cancer. Proc. Natl. Acad. Sci. U. S. A. 98, 14452–14457.

Vrljicak, P., Myburgh, D., Ryan, A.K., van Rooijen, M.A., Mummery, C.L.,

Gupta, I.R., 2004. Smad expression during kidney development. Am. J. Physiol.: Renal. Physiol. 286, F625–F633.
Wellik, D.M., Hawkes, P.J., Capecchi, M.R., 2002. Hox11 paralogous genes are essential for metanephric kidney induction. Genes Dev. 16, 1423–1432.
Yang, J., Mori, K., Li, J.Y., Barasch, J., 2003. Iron, lipocalin, and kidney epithelia. Am. J. Physiol.: Renal. Physiol. 285, F9–F18.
Yoshino, K., Rubin, J.S., Higinbotham, K.G., Uren, A., Anest, V., Plisov, S.Y., Perantoni, A.O., 2001. Secreted Frizzled-related proteins can regulate metanephric development. Mech. Dev. 102, 45–55.
Yu, J., Carroll, T.J., McMahon, A.P., 2002. Sonic hedgehog regulates proliferation and differentiation of mesenchymal cells in the mouse metanephric kidney. Development 129, 5301–5312.
Yu, J., McMahon, A.P., Valerius, M.T., 2004. Recent genetic studies of mouse kidney development. Curr. Opin. Genet. Dev. 14, 550–557.